

Critical properties of the Fermi-Bose Kondo and pseudogap Kondo models: Renormalized perturbation theory

Marijana Kirćan and Matthias Vojta

Institut für Theorie der Kondensierten Materie, Universität Karlsruhe, Postfach 6980, 76128 Karlsruhe, Germany

(Dated: Feb 10, 2004)

Magnetic impurities coupled to both fermionic and bosonic baths or to a fermionic bath with pseudogap density of states, described by the Fermi-Bose Kondo and pseudogap Kondo models, display non-trivial intermediate coupling fixed points associated with critical local-moment fluctuations and local non-Fermi liquid behavior. Based on renormalization group together with a renormalized perturbation expansion around the free-impurity limit, we calculate various impurity properties in the vicinity of those intermediate-coupling fixed points. In particular, we compute the conduction electron T matrix, the impurity susceptibility, and the residual impurity entropy, and relate our findings to certain scenarios of local quantum criticality in strongly correlated lattice models.

I. INTRODUCTION

Zero-temperature phase transitions in quantum impurity models have attracted significant interest in recent years in a number of different contexts. In correlated electron materials impurities have proven useful for investigating the complex bulk behavior, by probing the response to point defects e.g. in a spatially resolved manner by NMR or scanning-probe microscopy techniques. In quantum dot systems, impurity models naturally arise in describing the degrees of freedom on one or multiple dots together with their coupling to leads. Finally, the physics of strongly correlated bulk systems can be mapped to impurity models in the framework of the dynamical mean-field theory (DMFT)¹, where a local approximation to the lattice electron self-energy leads to an impurity model supplemented by a self-consistency condition.

Interesting transitions, where the zero-temperature behavior of the impurity degrees of freedom changes qualitatively as a function of some control parameter like coupling constants or gate voltages, occur in modifications of the familiar Kondo model, which describes an impurity spin interacting with conduction electrons of a metallic environment². Whereas the standard Kondo model does not show a phase transition at a finite value of the coupling, transitions naturally occur when other effects, which compete with fermionic Kondo screening, are added. At the resulting transition point, the Kondo energy scale is suppressed to zero, and the low-energy physics is dominated by critical local-moment fluctuations leading to singular thermodynamic properties and local non-Fermi liquid behavior. Notably, the physics at these intermediate-coupling fixed points is different from the well-studied multi-channel Kondo behavior.

In this paper, we will focus on two routes to impurity phase transitions. The first is represented by the so-called Fermi-Bose Kondo model^{3,4,5}, describing an impurity spin interacting with both fermionic quasiparticles and collective spin fluctuations. The Fermi-Bose Kondo model has recently been analyzed for the case of a metallic fermion density of states (DOS), and a gapless bosonic spectrum representing magnetic order pa-

rameter fluctuations at a bulk quantum critical point in d dimensions^{3,4,5}. For $d < 3$ the model shows an impurity quantum phase transition between a Kondo-screened phase and a bosonic fluctuating phase with universal local spin correlations. Recently, the Fermi-Bose Kondo model has been proposed⁶ to describe a “local quantum phase transition” in alloys like CeCu_{6-x}Au_x⁷. This modelling is based on an extended dynamical mean-field theory⁶, where the impurity site is coupled to both a fermionic and a bosonic self-consistent bath.

A second paradigmatic model is the pseudogap Kondo model^{8,9,10,11,12,13} where the fermionic bath displays a pseudogap DOS, $\rho_c(\omega) \propto |\omega|^r$. Such a bath arises in particular in ordered fermionic systems where the order parameter has nodes at the Fermi surfaces, like unconventional superconductors. In the pseudogap Kondo model, screening is suppressed for small Kondo couplings, and a transition between a Kondo-screened and a free-moment phase results. The pseudogap Kondo model has been extensively studied by a number of techniques, in particular using the numerical renormalization group method (NRG). Recently, it has become clear^{12,13} that $r = 0$ and $r = 1$ play the roles of the lower and upper-critical “dimensions”, respectively, allowing for different perturbative expansions to access the physics of the critical point. On the application side, the pseudogap Kondo effect is relevant for impurities in d -wave high-temperature superconductors, where indeed non-trivial Kondo-like behavior has been observed connected with the magnetic moments induced by Zn and Li impurities in YBa₂Cu₃O_{7- δ} ^{14,15,16}. Furthermore, it has been suggested¹⁷ that quantum dots coupled to interacting one-dimensional electron liquids can display pseudogap Kondo physics.

It is apparent that an analytical description of the properties near the intermediate-coupling fixed points is highly desirable to obtain a better understanding of the physics of critically fluctuating moments. In this paper we shall calculate a number of properties of the Fermi-Bose Kondo and the pseudogap Kondo models for parameters in the vicinity of the intermediate-coupling fixed points. These calculations are based on a perturbative renormalization group analysis of the models, together

with renormalized perturbation theory – this allows us to obtain results for observables in the quantum-critical regime where bare perturbation is known to diverge. As in earlier work^{3,4,5,18,19,20}, the expansion is done around the free-moment fixed point (which can be understood as expansion around the lower-critical dimension of the phase transitions). The small parameters controlling the perturbation theory are the exponents r and $\epsilon = 3 - d$ occurring in the fermionic and bosonic bath density of states, respectively. Critical properties will be computed in a double expansion in the non-linear couplings of the theory and the scaling dimensions r and ϵ . In particular, we will show that the impurity entropy is finite at the Fermi-Bose critical point, which has consequences for scenarios of local criticality in the framework of extended DMFT.

The paper is organized as follows. Sec. II will introduce the impurity models of interest and describe the properties of the fermionic and bosonic baths. In Sec. III we will briefly outline the renormalization group treatment which is based on a weak-coupling expansion of the impurity–bath couplings. In particular, all fixed points of the general pseudogap Fermi-Bose Kondo model will be enumerated and discussed. The calculation of observable impurity properties, namely susceptibility, entropy, and T matrix, is presented Secs. IV–VI. When possible, the results are compared with numerical data. Finally, Sec. VII discusses implications of our study for scenarios of local criticality in heavy-fermion metals. Technical details are relegated to the appendices; in addition we present a large- N calculation of the impurity entropy for the Bose Kondo model in App. D, which is not restricted small ϵ and thus complements the ϵ expansion of Sec. V.

Parts of the RG analysis and susceptibility calculations have been presented in Refs. 5,19,20,21; here we generalize these earlier works and derive additional results. The main new findings concern the impurity entropy, which, to our knowledge, has not been explicitly evaluated before and is an interesting property in the DMFT context; in addition, we present magnetic response results for the pseudogap Kondo model which can be nicely compared to numerical data.

II. MODELS

It is straightforward to combine the effects of a pseudogap bath and a competing bosonic interaction onto fermionic Kondo physics by considering the pseudogap Fermi-Bose Kondo model, which supersedes the variants discussed above. The Hamiltonian of the quantum impurity problem can be written as $\mathcal{H} = \mathcal{H}_c + \mathcal{H}_\phi + \mathcal{H}_{\text{imp}}$, with

$$\mathcal{H}_{\text{imp}} = \gamma_0 \hat{S}_\alpha \phi_\alpha(x=0) + j_0 \hat{S}_\alpha (c_\nu^\dagger \sigma_{\nu\mu}^{(\alpha)} c_\mu)(y=0). \quad (1)$$

Here, \hat{S} is the operator of the impurity spin, with $[\hat{S}_\alpha, \hat{S}_\beta] = i\epsilon_{\alpha\beta\gamma} \hat{S}_\gamma$, and we will restrict our attention

to $S = \frac{1}{2}$ in this paper. The fields $\phi_\alpha(x)$ and $c_\nu(y)$ describe bulk spin fluctuations and bulk fermionic excitations, respectively, with Hamiltonians \mathcal{H}_ϕ and \mathcal{H}_c to be discussed in the subsections below. In particular, the fermionic bath will follow a power law density of states,

$$\rho_c(\omega) \propto |\omega|^r, \quad (2)$$

which includes the cases of a metal ($r = 0$) and a d -wave superconductor ($r = 1$). ν, μ are spin indices with $\nu = \uparrow, \downarrow$, $\sigma^{(\alpha)}$ is the vector of Pauli spin matrices,

The impurity part of the Hamiltonian \mathcal{H}_{imp} , contains couplings to the bosonic and fermionic baths, characterized by coupling constants γ_0 and j_0 . In the absence of the bosonic bath, $\gamma_0 = 0$, and for $r = 0$ the model (1) reduces to the well-known Kondo model², which exhibits screening of the magnetic moment below a characteristic (Kondo) temperature, T_K . The pseudogap generalization, $r > 0$, shows a zero-temperature phase transition between a free local moment and a screened moment at a critical coupling $j_0 = j_{0c}$. On the other hand, in the absence of the fermionic bath, $j_0 = 0$, the Bose-Kondo model describes an impurity moment in an insulating quantum antiferromagnet^{18,19,21}; in addition it arises in mean-field theories for spin liquids and spin glasses²². Our analysis will be restricted to a model with full rotation symmetry in spin space; the effect of spin anisotropy for $r = 0$ has been discussed in Ref. 5.

A. Fermionic bath

The fermionic bath consists of non-interacting spin- $\frac{1}{2}$ fermions. (More precisely, the fermionic self-interaction is assumed to be irrelevant in the RG sense.) A convenient continuum representation uses chiral fermions with a linear dispersion in $(1 + r)$ dimensions:

$$\mathcal{H}_c = \int dk |k|^r (v_F k) c_{k\nu}^\dagger c_{k\nu}. \quad (3)$$

The field $c_\nu(y = 0)$ in Eq. (1) is simply the Fourier transform of $c_{k\nu}$, $c_\nu(y = 0) = \int dk |k|^r c_{k\nu}$. The velocity v_F will be set to unity in the following.

We assume particle-hole symmetry of the bath; in the applicability range of our expansion particle-hole symmetry breaking is marginal for $r = 0$ and irrelevant for $r > 0$ and thus does not change our conclusions. As will be mentioned in Sec. III, particle-hole symmetry breaking becomes important for larger r and/or in the strong-coupling regime.

In d -wave superconductors, $r = 1$, and the c fermions represent the superconducting Bogoliubov quasiparticles in the vicinity of the nodes of the d -wave gap.

B. Bosonic bath

The bosonic bath, representing antiferromagnetic spin-1 collective fluctuations of the host material, will be de-

scribed by the O(3)-symmetric quantum ϕ^4 theory in d dimensions,

$$\mathcal{H}_\phi = \int d^d x \left[\frac{\pi_\alpha^2 + c^2 (\nabla_x \phi_\alpha)^2 + s \phi_\alpha^2}{2} + \frac{g_0}{4!} (\phi_\alpha^2)^2 \right], \quad (4)$$

where the field $\phi_\alpha(x)$ represents the local orientation and magnitude of the (non-conserved) antiferromagnetic order parameter, and its canonically conjugate momentum is $\pi_\alpha(x)$, hence $[\phi_\alpha(x), \pi_\beta(x')] = i\delta_{\alpha\beta}\delta^d(x-x')$. The parameter s tunes a quantum transition between a paramagnetic phase for $s > s_c$ and an ordered phase breaking the O(3) symmetry at $s < s_c$. g_0 is the self-interaction of the ϕ quanta, and c is a velocity, and we will use units such that $c = 1$ in the following. The phase transition of the ϕ^4 theory can be studied by working in $(3-\epsilon)$ space dimensions, using a perturbative expansion in ϵ .

The quantum paramagnet for $s > s_c$ is characterized by its spin gap Δ_s at $T = 0$, and this vanishes as s approaches s_c from above as

$$\Delta_s \propto (s - s_c)^{\nu_\phi} \quad (5)$$

where ν_ϕ is the correlation length exponent of the magnetic bulk transition described by \mathcal{H}_ϕ ; the dynamical exponent is $z = 1$. The local two-point ϕ_α propagator in imaginary time τ is given by

$$\begin{aligned} D_\phi(\tau) &= \langle \phi_\alpha(0, \tau) \phi_\alpha(0, 0) \rangle_0 \\ &= T \sum_{\omega_n} \int \frac{d^d k}{(2\pi)^d} \frac{e^{-i\omega_n \tau}}{\omega_n^2 + k^2 + m^2}. \end{aligned} \quad (6)$$

Here the momentum k is measured relative to the ordering wavevector \mathbf{Q} of the magnet. The 0 subscript in the correlator indicates that it is evaluated to zeroth order in g_0 . However, we have included Hartree-Fock renormalizations in the determination of the ‘‘mass’’ m ; these have been computed in earlier work in the ϵ expansion²³, and we quote some limiting cases to lowest order in $\epsilon = 3 - d$:

$$m = \begin{cases} \Delta_s & ; \quad s \geq s_c, \quad T \ll \Delta_s \\ \sqrt{10\epsilon/33} \pi T & ; \quad T \gg |s - s_c|^{\nu_\phi} \end{cases}. \quad (7)$$

It is useful to define a spectral density, $\rho_\phi(\omega)$, of the Bose field ϕ . At $T = 0$ it will display a gap of size Δ_s ; for $\Delta_s = 0$ it follows $\rho_\phi(\omega) \propto \text{sgn}(\omega)|\omega|^{1-\epsilon}$.

For $d < 3$ the bosonic self-interaction g_0 is relevant in the RG sense and cannot be neglected. However, in the RG analysis of the impurity model (1), modifications from g_0 arise only at two-loop order. Treatments of the Fermi-Bose Kondo model in the context of extended DMFT^{5,6} worked with a $g_0 = 0$ theory – there the irrelevance of the bosonic self-interactions was argued to be justified due to the Landau damping of the spin fluctuations. In what follows, we will treat both $g_0 = 0$ and $g_0 \neq 0$ simultaneously, and display all results for both cases. In applications, the $g_0 \neq 0$ case is relevant in the absence of Landau damping of the spin fluctuations, i.e., for metallic systems with a small Fermi surface obeying $|\mathbf{Q}| > 2k_F$ and for pseudogap systems like d -wave superconductors¹⁹.

III. RENORMALIZATION GROUP

The Fermi-Bose Kondo model (1) can be conveniently analyzed using standard renormalization group techniques. We shall assume that the spectrum of the bosonic bath is gapless, $\Delta_s = 0$ at $T = 0$, which corresponds to a magnetic bulk quantum critical point. Then, both fermionic and bosonic baths obey a power law DOS. The RG can be formulated as expansion in the bath exponents ϵ and r , similar to Refs. 3,5,18,19.

It proves convenient to switch from the spin operators for the impurity in (1) to an Abrikosov pseudo-fermion representation of the impurity spin $\frac{1}{2}$, $\vec{S} = f_\nu^\dagger \vec{\sigma}_{\nu\mu} f_\mu$. The required Hilbert space constraint $f_\nu^\dagger f_\nu = \hat{Q} = 1$ will be implemented using a chemical potential $\lambda \rightarrow \infty$, such that observables $\langle \hat{O} \rangle$ have to be calculated according to^{24,25}

$$\langle \hat{O} \rangle = \lim_{\lambda \rightarrow \infty} \frac{\langle \hat{Q} \hat{O} \rangle_\lambda}{\langle \hat{Q} \rangle_\lambda}, \quad (8)$$

where $\langle \dots \rangle_\lambda$ denotes the thermal expectation value calculated using pseudo-fermions in the presence of the chemical potential λ . Clearly, in the limit $\lambda \rightarrow \infty$ the term $\langle \hat{Q} \rangle_\lambda$ represents the partition function of the physical sector of the Hilbert space times $\exp(-\lambda\beta)$. As detailed in App. B, both numerator *and* denominator of Eq. (8) have to be expanded in the non-linear couplings to the required order when calculating observables; however, the denominator does typically not develop logarithmic singularities at the marginal dimension.

As an alternative to the pseudo-fermion technique, the approach of Ref. 19 can be utilized, which does not employ pseudo-fermions, and is completely equivalent for the present single-impurity problem.

A. RG transformation

Some crucial properties of the partition function $Z = \text{Tr} e^{-\beta\mathcal{H}}$ follow from tree-level power-counting. The behavior of the fields under a rescaling transformation determines the scaling dimensions:

$$\begin{aligned} \dim[\phi_\alpha] &= (d-1)/2; & \dim[c_\nu] &= (1+r)/2; \\ \dim[f_\nu] &= 0. \end{aligned} \quad (9)$$

The last line refers to the pseudo-fermion representation of the impurity spin. The above can be used to determine the dimensions of the couplings:

$$\begin{aligned} \dim[g_0] &= 3-d; \\ \dim[\gamma_0] &= (3-d)/2; & \dim[j_0] &= -r. \end{aligned} \quad (10)$$

Thus, the bosonic bulk interaction g_0 is relevant for $d < 3$, i.e., the bulk critical point will be characterized by a finite fixed point value of g . The bosonic impurity coupling γ_0 is a relevant perturbation about the decoupled

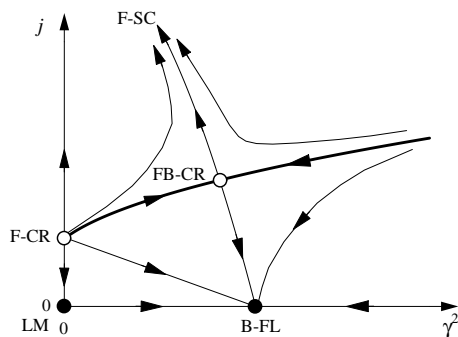


FIG. 1: Schematic RG flow diagram for the pseudogap Fermi-Bose Kondo model for small ϵ and r , and $\Delta_s = 0$, deduced from the beta functions (12), (A11). The horizontal axis denotes the coupling to the bosonic bath, γ , the vertical axis denotes the fermionic Kondo coupling, j . The solid dots are (meta)stable fixed points, the open dots denote critical fixed points, the thick line is the separatrix, for details see text.

impurity fixed point in $d < 3$ – this will yield a *stable* fixed point with finite $\gamma^{4,18,19}$. In contrast, the fermionic coupling j_0 is irrelevant, which eventually results in an *unstable* fixed point describing the phase transition in the pseudogap Kondo model. The combined effect of γ_0 and j_0 will be captured in the following RG treatment.

To one-loop order, the familiar momentum shell method with ultra-violet (UV) cutoff Λ can be employed; the field-theoretic RG calculation to two-loop order will be sketched in App. A. Within the momentum shell scheme, dimensionless couplings are introduced as $g_0 = g\Lambda^\epsilon/S_{d+1}$, $j_0 = j\Lambda^{-r}$, $\gamma_0 = \gamma\Lambda^{\epsilon/2}/\tilde{S}_{d+1}^{1/2}$ with the phase space factors S_d , \tilde{S}_d defined in Eq. (A6). Without loss of generality the same value of the UV cutoff can be used for the fermionic and bosonic subsystems. The RG for the bulk bosonic theory gives

$$\beta(g) = -\epsilon g + \frac{11g^2}{6}. \quad (11)$$

For the impurity part, the one-loop RG result for the beta functions is

$$\begin{aligned} \beta(\gamma) &= -\frac{\epsilon\gamma}{2} + \gamma^3, \\ \beta(j) &= rj - j^2 + j\gamma^2, \end{aligned} \quad (12)$$

the two-loop results can be found in App. A in Eq. (A11). Already at one-loop level, a term mixing j and γ appears, which determines the competition between fermionic and bosonic Kondo coupling. The resulting RG flow in the j - γ plane is shown in Fig. 1, the fixed points will be discussed in the following subsection.

The equations (12), (A11) reduce to the cases of the pseudogap Kondo model for $\gamma = 0$ (Ref. 8), the Bose-Kondo model for $j = 0$ (Ref. 19), and the metallic Fermi-Bose Kondo model with non-interacting bosons for $r = 0$ and $g = 0$ (Refs. 4,5).

B. Fixed points

In the following we list the RG fixed points, obtained from (A11), and quote some of their observable properties like the Curie part of impurity susceptibility $T\chi_{\text{imp}}$ and the residual impurity entropy S_{imp} ; details of the calculation appear in Secs. IV and V.

1. Local-moment fixed point (LM)

The decoupled impurity fixed point is simply characterized by $\gamma^* = j^* = 0$. The susceptibility shows the full Curie moment of a spin $\frac{1}{2}$, $T\chi_{\text{imp}} = 1/4$, and the impurity entropy is $S_{\text{imp}} = \ln 2$.

2. Fermionic strong-coupling fixed point (F-SC)

For large fermionic Kondo coupling j , the bosonic part γ is irrelevant, and the model reduces to the fermionic pseudogap Kondo model which shows strong-coupling phases with screening ($j^* = \infty$, $\gamma^* = 0$). This regime is not accessible within the present perturbation expansion, and we just quote the known results for the Kondo model. For the metallic case, $r = 0$, there is a line of strong-coupling fixed points parametrized by particle-hole asymmetry, along this line $T\chi_{\text{imp}} = 0$ and $S_{\text{imp}} = 0$. In contrast, for $r > 0$ two different strong-coupling fixed points exist¹¹. The particle-hole symmetric one is unstable w.r.t. particle-hole symmetry breaking and only accessible for $r < 1/2$, it does not display complete screening: the susceptibility follows $T\chi_{\text{imp}} = r/8$, and the impurity entropy is $S_{\text{imp}} = 2r \ln 2$. In contrast, the asymmetric strong-coupling fixed point is stable and exists for all $r > 0$, with $T\chi_{\text{imp}} = 0$ and $S_{\text{imp}} = 0$.

3. Bosonic fluctuating fixed point (B-FL)

In the absence of a fermionic bath, the Bose Kondo problem shows interesting behavior: it flows to a stable intermediate-coupling fixed point, characterized by

$$\begin{aligned} \gamma^{*2} &= \begin{cases} \frac{\epsilon}{2} + \epsilon^2 \left(\frac{29}{121} - \frac{5\pi^2}{132} \right) + \mathcal{O}(\epsilon^3) & \text{for } g_0 \neq 0 \\ \frac{\epsilon}{2} + \frac{\epsilon^2}{4} + \mathcal{O}(\epsilon^3) & \text{for } g_0 = 0 \end{cases} \\ j^* &= 0. \end{aligned} \quad (13)$$

At this fixed point the fermionic Kondo coupling j is irrelevant. The intermediate-coupling nature leads to universal local-moment fluctuations^{18,19}, with $T\chi_{\text{imp}} > 0$ and $0 < S_{\text{imp}} < \ln 2$. The anomalous dimension of the

auxiliary impurity fermionic field (see also App. A) is

$$\eta_f = \begin{cases} \frac{3\epsilon}{8} - \frac{3\epsilon^2}{8} \left(\frac{5}{242} + \frac{5\pi^2}{66} \right) + \mathcal{O}(\epsilon^3) & \text{for } g_0 \neq 0 \\ \frac{3\epsilon}{8} + \mathcal{O}(\epsilon^3) & \text{for } g_0 = 0 \end{cases}. \quad (14)$$

η_f describes the decay of the two-point correlator of the f fermions. In the Kondo model (1) this propagator is not directly measurable; however, it has been argued²⁶ that mobile fermionic quasiparticles in a critical antiferromagnet are described by a very similar theory, provided that their momentum is close to a minimum or van-Hove point of the band structure, such that the dispersion is quadratic and can be neglected. Then, η_f is the exponent of the electron Green's function as measured in photoemission:

$$G_e \propto \frac{1}{(\omega - \epsilon_0)^{1-\eta_f}}, \quad (15)$$

where ϵ_0 is the (renormalized) energy of the quasiparticle. This situation, which can be regarded as the bosonic analogue of the familiar x-ray edge problem²⁷, applies to electrons in Kondo insulators at a magnetic critical point, and could also be relevant for holes near the anti-nodal points in high-temperature superconductors²⁶.

As noted earlier^{5,19} the B-FL fixed point is unstable w.r.t. breaking of the spin rotation symmetry. Further, for $\epsilon \rightarrow 0$ it merges with LM.

4. Fermionic critical fixed point (F-CR)

The pure fermionic problem with a pseudogap, $r > 0$, features a critical fixed point with

$$j^* = r + \frac{r^2}{2} + \mathcal{O}(r^3), \quad \gamma^* = 0 \quad (16)$$

which controls the transition between the decoupled and the Kondo-screened phases. As detailed below, we have $0 < T\chi_{\text{imp}} < 1/4$ and $S_{\text{imp}} > \ln 2$. The anomalous field dimension is given by

$$\eta_f = \frac{3r^2}{8} + \mathcal{O}(r^3). \quad (17)$$

As the fixed point is infrared unstable, we can discuss the scaling dimension of the leading relevant operator, which is just the inverse correlation length exponent of the LM – F-SC transition. Expanding the beta function around the fixed point value yields:

$$\frac{1}{\nu} = r - \frac{r^2}{2} + \mathcal{O}(r^3). \quad (18)$$

This exponent describes the vanishing of the characteristic energy scale T^* when the system is tuned through the transition, i.e., $T^* \propto |j_0 - j_{0c}|^\nu$.

The F-CR fixed point is unstable w.r.t a finite coupling to gapless bosons, therefore it cannot be reached

for $\gamma_0 \neq 0$ if $\Delta_s = 0$. The flow diagram, Fig. 1 shows that F-CR can be understood as a multicritical fixed point; consequently, universal one-parameter scaling in its vicinity is only realized for $\gamma_0 = 0$. For $r \rightarrow 0$, the F-CR fixed point merges with LM.

NRG calculations¹¹ have established that the fixed-point structure of the pseudogap Kondo problem changes for larger r , and two different critical fixed points occur for $r > r^* \approx 0.375$. The particle-hole symmetric critical fixed point, present at small r , disappears for $r \geq \frac{1}{2}$. Notably, the particle-hole symmetric and asymmetric critical fixed points share many common properties^{11,12,13}. In any case, the physics at large r is inaccessible within the present weak-coupling expansion; we will restrict our attention to the range of $0 < r < \frac{1}{2}$ in the following.

5. Fermi-Bose critical fixed point (FB-CR)

Finally, the FB-CR fixed point controls the transition between F-SC and B-FL, i.e., between the phase with fermionic screening and the bosonic fluctuating phase. For interacting bosons, $g_0 \neq 0$, we have

$$\begin{aligned} \gamma^{*2} &= \frac{\epsilon}{2} + \epsilon^2 \left(\frac{111}{968} - \frac{5\pi^2}{132} \right) - \frac{\epsilon r}{2} - \frac{r^2}{2} + \mathcal{O}(\epsilon, r)^3, \\ j^* &= r + \frac{\epsilon}{2} - \epsilon^2 \left(\frac{5}{484} + \frac{5\pi^2}{132} \right) + \mathcal{O}(\epsilon, r)^3 \end{aligned} \quad (19)$$

whereas for $g = 0$ we find

$$\begin{aligned} \gamma^{*2} &= \frac{\epsilon}{2} + \frac{\epsilon^2}{8} - \frac{\epsilon r}{2} - \frac{r^2}{2} + \mathcal{O}(\epsilon, r)^3, \\ j^* &= r + \frac{\epsilon}{2} + \mathcal{O}(\epsilon, r)^3. \end{aligned} \quad (20)$$

The fixed point is again characterized by non-trivial universal values of $T\chi_{\text{imp}}$ and S_{imp} depending on r and ϵ only, in particular for $r = 0$ we have $0 < S_{\text{imp}} < \ln 2$. The anomalous field dimension is

$$\eta_f = \begin{cases} \frac{3\epsilon}{8} - \frac{3\epsilon^2}{8} \left(\frac{5}{242} + \frac{5\pi^2}{66} \right) + \mathcal{O}(\epsilon, r)^3 & \text{for } g_0 \neq 0 \\ \frac{3\epsilon}{8} + \mathcal{O}(\epsilon, r)^3 & \text{for } g_0 = 0 \end{cases}. \quad (21)$$

The inverse correlation length exponent of the B-FL – F-SC transition is

$$\frac{1}{\nu} = \begin{cases} r + \frac{\epsilon}{2} - \epsilon^2 \left(\frac{34}{363} + \frac{5\pi^2}{132} \right) - \frac{4\epsilon r}{9} - \frac{19r^2}{27} & \text{for } g_0 \neq 0 \\ r + \frac{\epsilon}{2} - \frac{\epsilon^2}{12} - \frac{4\epsilon r}{9} - \frac{19r^2}{27} & \text{for } g_0 = 0 \end{cases} \quad (22)$$

up to terms of order $\mathcal{O}(\epsilon, r)^3$. Note that this exponent describes the behavior if the impurity model is tuned off criticality by varying j_0 or γ_0 , while maintaining criticality of the bulk magnet (!), $\Delta_s = 0$. If, in contrast, the bosonic bath is tuned away from its critical point, then the physics is dominated by Δ_s (5), as discussed in Ref. 19 (see also Sec. III D below). The FB-CR fixed point only exists for $\epsilon > 0$.

The results of Refs. 11,13 suggest that the fixed point character of FB-CR changes for larger r similar to that of the F-CR fixed point. In contrast, the properties of the bosonic part are likely smooth as function of ϵ for $0 < \epsilon < 2$ ($1 < d < 3$), as the $(1 + \epsilon)$ expansion of Ref. 28 yields universal properties similar to the $(3 - \epsilon)$ expansion¹⁹; this is further supported by the large- N theory presented in Ref. 19 and App. D.

C. Phase diagram

The schematic RG flow from this small (ϵ, r) analysis is shown in Fig. 1. The main conclusion is that the fermionic and bosonic Kondo couplings compete, i.e., the coupling of an impurity to collective spin fluctuations suppressed fermionic Kondo screening. This can be an important aspect for impurity moments in strongly correlated materials²⁰.

We expect the general structure of the phase diagram to be valid for all values $0 < \epsilon < 2$ and $r > 0$. This is suggested by numerics for the fermionic part^{10,11} and various large- N methods^{19,20}; for $r > \frac{1}{2}$ particle-hole asymmetry is needed to reach the F-SC fixed point as noted above. For the case of a metallic fermionic bath, $r = 0$, the F-CR fixed point is absent, and the phase transition line originates in the $\gamma = j = 0$ point, see Refs. 4,5.

D. Tuning bulk vs. boundary criticality

So far the analysis was restricted to $s = s_c$, i.e., the bulk quantum critical point of the host magnet; here we have seen that tuning the couplings j_0 and γ_0 can lead to boundary quantum phase transitions.

It is instructive to also discuss the physics away from the bulk critical point, and in particular the behavior of the impurity properties upon tuning the *bulk* magnet through its ordering transition. The behavior will of course depend on whether the values of the impurity couplings, j_0 and γ_0 , place the impurity problem at $s = s_c$ into the F-SC or B-FL phases, or on the phase transition line, Fig. 1.

1. $r = 0$

For the metallic case, $r = 0$, a finite host spin gap, corresponding to $s > s_c$, always leads to an impurity screened by fermionic quasiparticles.

Then, for large j_0 there is no qualitative change in the impurity properties when tuning $(s - s_c)$ through zero, because for $s < s_c$ the physics is described by a screened Kondo impurity in a weak magnetic field². In contrast, for small j_0 the low-energy behavior of the impurity changes from F-SC for $s > s_c$ to B-FL at $s = s_c$, and for $s < s_c$ the moment is polarized by the exchange field, with an effective magnetization $\propto (s_c - s)^{\nu_\phi \eta_\times / 2}$

(Ref. 19). Only for j_0, γ_0 placing the impurity problem on the transition line in Fig. 1, the impurity is driven critical by driving the bulk to the critical point.

2. $r > 0$

In the pseudogap situation, $r > 0$, the presence of a finite host spin gap, $\Delta_s > 0$, still allows a transition between LM and F-SC. This can be understood in a two-step RG procedure: For UV cutoff energies larger than Δ_s the above RG can be applied, generating a flow of j . Once the UV cutoff reaches Δ_s , the RG flow of γ is terminated. The remaining RG procedure then effectively treats a model with fermionic bath only, but the flow of j starts at $j(\Delta_s)$ generated in the first part of the RG. Thus for $r > 0$ there exists a transition between LM and F-SC as function of j_0 , controlled by the F-CR fixed point.

We can now discuss the behavior when tuning the bulk magnet through its critical point. For large j_0 the impurity is screened, and its properties remain essentially unchanged upon tuning $(s - s_c)$ through zero as above. For very small j_0 the low-energy behavior of the impurity changes now from LM (!) for $s > s_c$ to B-FL at $s = s_c$, and at $s < s_c$ the moment is polarized. Interestingly, there is now a significant intermediate range of j_0 values where the impurity is screened for large Δ_s , then becomes uncrened for smaller Δ_s (Ref. 20) – this transition is the one controlled by F-CR – and at $s \leq s_c$ the behavior again is determined by B-FL¹⁹.

Summarizing this discussion, for the single-impurity model it is clear that, for generic values of the impurity couplings j_0 and γ_0 , tuning the bulk magnet critical does *not* drive the impurity problem critical; coincidence of the two critical points requires additional fine tuning of parameters.

IV. MAGNETIC SUSCEPTIBILITY

The linear response functions to an applied field have been discussed for the purely bosonic model in Ref. 19; here we supplement this by calculating the fermionic contributions and collecting the results for the different fixed points. Also, we briefly discuss hyperscaling properties with respect to a local field near the critical fixed points.

The external field is coupled to the bulk magnetic degrees of freedom using the following replacement in \mathcal{H}_ϕ ,

$$\pi_\alpha^2 \rightarrow (\pi_\alpha - i\epsilon_{\alpha\beta\gamma} H_{u\beta}(x)\phi_\gamma)^2, \quad (23)$$

while we simply add field terms to \mathcal{H}_c and \mathcal{H}_{imp} ,

$$\begin{aligned} & -H_{u\alpha}(y)(c_\nu^\dagger \sigma_{\nu\mu}^\alpha c_\mu)(y) \text{ and} \\ & -H_{\text{imp},\alpha} \hat{S}_\alpha. \end{aligned} \quad (24)$$

The bulk field H_u varies slowly as function of the space coordinate, and H_{imp} is the magnetic field at the location of the impurity.

With these definitions, a spatially uniform field applied to the whole system corresponds to $H_u = H_{\text{imp}} = H$. Response functions can be defined from second derivatives of the thermodynamic potential, $\Omega = -T \ln Z$, in the standard way¹⁹: $\chi_{u,u}$ measures the bulk response to a field applied to the bulk, $\chi_{\text{imp,imp}}$ is the impurity response to a field applied to the impurity, and $\chi_{u,\text{imp}}$ is the cross-response of the bulk to an impurity field. Then the impurity contribution to the total susceptibility is defined as

$$\chi_{\text{imp}}(T) = \chi_{\text{imp,imp}} + 2\chi_{u,\text{imp}} + (\chi_{u,u} - \chi_{u,u}^{\text{bulk}}), \quad (25)$$

where $\chi_{u,u}^{\text{bulk}}$ is the susceptibility of the bulk system in absence of impurities. The local impurity susceptibility is given by

$$\chi_{\text{loc}}(T) = \chi_{\text{imp,imp}}, \quad (26)$$

which is equivalent to the zero-frequency impurity spin autocorrelation function.

A. Local susceptibility

The local susceptibility $\chi_{\text{loc}}(T)$ at an intermediate-coupling fixed point is expected to follow a power law,

$$\lim_{T \rightarrow 0} \chi_{\text{loc}}(T) \propto \frac{1}{T^{1-\eta_\chi}}. \quad (27)$$

This relation defines an anomalous exponent, η_χ , which controls the anomalous decay of the two-point correlations of the impurity spin. (In Refs. 19,21 this exponent was labelled η' .)

Following the standard scheme²⁹, η_χ is calculated by introducing a χ_{loc} renormalization factor, Z_χ , evaluating the lowest-order diagrams for χ_{loc} , and demanding the resulting renormalized expression to be free of poles. From the two-loop expression for Z_χ , given in App. A, we find $\eta_\chi = 2(\gamma^2 - \gamma^4) + j^2$. Evaluating this at the RG fixed points yields

$$\text{F-CR: } \eta_\chi = r^2 + \mathcal{O}(r^3), \quad (28)$$

$$\text{FB-CR: } \eta_\chi = \epsilon - \epsilon^2 \left(\frac{5}{242} + \frac{5\pi^2}{66} \right) + \mathcal{O}(\epsilon, r)^3,$$

$$\text{B-FL: } \eta_\chi = \epsilon - \epsilon^2 \left(\frac{5}{242} + \frac{5\pi^2}{66} \right) + \mathcal{O}(\epsilon^3),$$

where the last two lines are for interacting bosons. We see no reason that the η_χ values for the FB-CR and B-FL fixed points should be equal to all orders. In contrast, for non-interacting bosons, $g = 0$, it has been shown in Refs. 5,19 that all higher-order corrections to η_χ vanish identically at a fixed point with finite γ^* , thus

$$\text{FB-CR: } \eta_\chi = \epsilon, \quad (29)$$

$$\text{B-FL: } \eta_\chi = \epsilon$$

to all orders in perturbation theory. To the order we have worked here we find $\eta_f = 3\eta_\chi/8$, but this does not hold to higher orders.

B. Hyperscaling

The structure of the RG implies that the impurity correlations obey certain hyperscaling properties at the non-trivial fixed points, including ω/T scaling in dynamical quantities³⁰. For instance, the dynamic local susceptibility at criticality obeys

$$\chi''_{\text{loc}}(\omega, T) = \frac{\mathcal{B}_1}{\omega^{1-\eta_\chi}} \Phi_1\left(\frac{\omega}{T}\right), \quad (30)$$

where Φ_1 is a universal crossover function (for the particular fixed point), and \mathcal{B}_1 is a non-universal prefactor. The asymptotic behavior of $\Phi_1(x)$ is

$$\Phi_1(x) = \begin{cases} x^{1-\eta_\chi} & \text{for } x \rightarrow 0 \\ \text{const} & \text{for } x \rightarrow \infty \end{cases}. \quad (31)$$

A similar scaling form applies for the T matrix, see below.

In addition, for the critical fixed points F-CR and FB-CR we can also consider scaling properties away from, but close to, criticality. For details in the context of the pseudogap Kondo model we refer the reader to Ref. 12. In particular, the static local susceptibility follows

$$\chi_{\text{loc}}(T) = \frac{\mathcal{B}_2}{T^{1-\eta_\chi}} \Phi_2\left(\frac{T^{1/(\nu)}}{j_0 - j_{0c}}\right). \quad (32)$$

Using hyperscaling, the results for the correlation length exponent ν , Sec. III, and for the anomalous exponent η_χ from above are sufficient to determine all critical exponents associated with a local magnetic field¹². In particular, the $T \rightarrow 0$ local susceptibility away from criticality obeys:

$$\begin{aligned} \chi_{\text{loc}}(j_0 > j_{0c}) &\propto (j_0 - j_{0c})^{-\bar{\gamma}}, \quad \bar{\gamma} = \nu(1 - \eta_\chi), \\ T\chi_{\text{loc}}(j_0 < j_{0c}) &\propto (j_{0c} - j_0)^{\bar{\gamma}'}, \quad \bar{\gamma}' = \nu\eta_\chi. \end{aligned} \quad (33)$$

With these definitions, the exponents $\bar{\gamma}$ and $\bar{\gamma}'/2$ coincide with the exponents γ and β defined in Ref. 12. The perturbative expressions for the exponents in Eq. (33) are

$$\begin{aligned} \text{F-CR: } \bar{\gamma} &= \frac{1}{r} + \frac{1}{2} + \mathcal{O}(r), \\ \bar{\gamma}' &= r + \mathcal{O}(r^2), \\ \text{FB-CR: } \bar{\gamma} &= \frac{2}{2r + \epsilon} + \mathcal{O}(1), \\ \bar{\gamma}' &= \frac{2\epsilon}{2r + \epsilon} + \mathcal{O}(\epsilon, r). \end{aligned} \quad (34)$$

At this order the results for $g = 0$ and $g \neq 0$ are identical; the next-to-leading order contributions at the FB-CR fixed point can also be found from (22). The results for the F-CR fixed point can be compared with numerical results¹², with excellent agreement, e.g., $\bar{\gamma}(r = 0.1) = 10.63 \pm 0.02$ from NRG, see also Fig. 2.

As proposed earlier^{11,12}, $\lim_{T \rightarrow 0} T\chi_{\text{loc}}$ can serve as an order parameter, as it vanishes continuously as $j_0 \rightarrow j_{0c}$ from below, and is zero for $j_0 > j_{0c}$, i.e., in the F-SC phase.

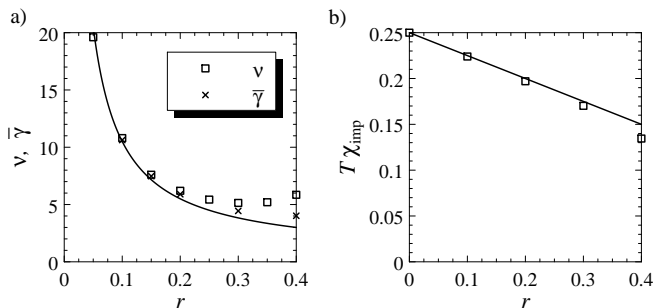


FIG. 2: Comparison of numerical data for the critical point of the pseudogap Kondo model (F-CR), obtained with NRG, to the analytical results of the renormalized perturbation theory. a) Correlation length exponent ν and susceptibility exponent $\bar{\gamma}$ (33). The analytical results are in (18) and (34): to two-loop order, both exponents are equal, and shown by the solid line. The symbols are NRG data from Refs. 10,12. b) Curie prefactor C_{imp} of the impurity susceptibility (35). Solid: analytical result (39); squares: NRG data taken from Ref. 11.

C. Impurity susceptibility

The quantity χ_{imp} measures the impurity contribution to the total uniform susceptibility. Importantly, it does not acquire an anomalous dimension at an intermediate-coupling fixed point²³, because it is a response function associated to the conserved quantity S_{tot} . Thus we expect a Curie law

$$\lim_{T \rightarrow 0} \chi_{\text{imp}}(T) = \frac{C_{\text{imp}}}{T}, \quad (35)$$

where the prefactor is in general a non-trivial universal constant different from the free-impurity value $S(S+1)/3$. Apparently, Eq. (35) can be interpreted as the Curie response of a fractional effective spin¹⁸.

Since the present expansion is done around the free-impurity fixed point of the $S = \frac{1}{2}$ impurity, the result will always have the form $T\chi_{\text{imp}} = \frac{1}{4} + \Delta(T\chi_{\text{imp}})$. Technically, the absence of an anomalous dimension implies that no poles in ϵ or r will appear in the perturbative expression for χ_{imp} , i.e., all poles from the different contributions have to cancel. Importantly, such pole-free contributions can also arise from the denominator in Eq. (8), see App. B.

At this point a reference to the two-channel Kondo problem is in order, where it is known that χ_{imp} *does* display an anomalous power law. This does not contradict the above statement, however, in the two-channel model the prefactor C_{imp} of Eq. (35) actually vanishes due to a ‘‘compensation’’ effect³¹, and the leading low-temperature behavior arises from corrections to scaling^{32,33}.

Proceeding with our calculation, we first focus on the fermionic part. The analysis of χ_{loc} has shown that the first corrections to free-moment behavior arise at order j_0^2 . This is different for χ_{imp} : there is a single diagram

proportional to j_0 which contributes to $\chi_{\text{u,imp}}$:

$$\chi_{\text{u,imp}} = -j_0 \frac{1}{4T^2} \int dk |k|^r \frac{\cosh^{-2}(k/2T)}{4} \quad (36)$$

Evaluating the integral in the limit of infinite UV cutoff and taking $r \rightarrow 0$ gives:

$$\Delta(T\chi_{\text{imp}})^{(f)} = -\frac{j}{4} \quad (37)$$

where we have already expressed the result in terms of the renormalized coupling j , $j_0 = j\mu^{-r}$, and used $(T/\mu)^r = 1 + \mathcal{O}(r)$.

The bosonic contributions have been discussed in Ref. 19; here we only quote the result for completeness. Importantly, the impurity susceptibility is not a well-defined quantity for non-interacting bosons ($g = 0$) because the application of a uniform field would lead to negative bosonic mode energies – this yields an infrared singular magnetic response of the bulk system, and a similar infrared singularity of $T\chi_{\text{imp}}$. For interacting bosons, the lowest-order term gives¹⁹

$$\Delta(T\chi_{\text{imp}})^{(b_{\text{int}})} = \frac{1}{4} \sqrt{\frac{33}{10\epsilon}} \gamma^2 \quad (38)$$

where the Hartree-Fock renormalization of the mass (7) is required to remove the infrared divergence of the integral.

With these perturbative results, we can finally evaluate the impurity susceptibility at the intermediate-coupling fixed points, to lowest non-trivial order. For the bosonic part, the order ϵ contribution can also be identified¹⁹.

$$\text{F-CR} : T\chi_{\text{imp}} = \frac{1}{4}(1-r) + \mathcal{O}(r^2), \quad (39)$$

$$\text{FB-CR} : T\chi_{\text{imp}} = \frac{1}{4} \left(1 + \sqrt{\frac{33\epsilon}{40}} - \frac{9\epsilon}{4} - r \right) + \mathcal{O}(\epsilon^{3/2}, \epsilon^{1/2}r),$$

$$\text{B-FL} : T\chi_{\text{imp}} = \frac{1}{4} \left(1 + \sqrt{\frac{33\epsilon}{40}} - \frac{7\epsilon}{4} \right) + \mathcal{O}(\epsilon^{3/2}).$$

Notably, our result for the F-CR fixed point is in excellent agreement with the NRG of Ref. 11, see Fig. 2.

For the bosonic case no numerical results for small ϵ are available; calculations³⁴ for $\epsilon = 1$ ($d = 2$) have found a value for $T\chi_{\text{imp}}$ which is very close to the free-moment value $\frac{1}{4}$. We believe that this coincidence is due to large corrections from higher orders of the ϵ expansion; the fact that our result for the fermionic F-CR fixed point agrees well with numerics strongly supports that the renormalized perturbation expansion employed here is the correct method to evaluate the impurity susceptibility (which had been questioned in Ref. 35).

V. IMPURITY ENTROPY

In general, zero-temperature critical points in quantum impurity models can show a finite residual entropy

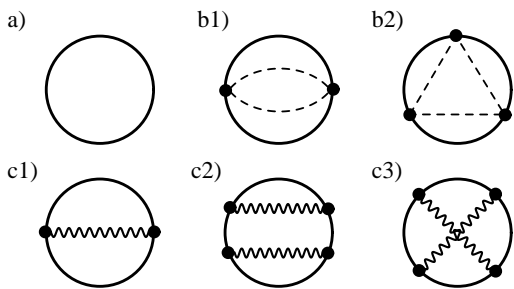


FIG. 3: Feynman diagrams for the impurity partition function of the physical sector of the Hilbert space, i.e., $\langle \hat{Q} \rangle_\lambda$. These diagrams directly enter the calculation of the impurity entropy. Full/dashed/wiggly lines denote $f/c/\phi$ propagators, and the dots are the interaction vertices. a) Unperturbed impurity part. b) and c) Corrections from the fermionic and bosonic baths.

– this is in contrast to bulk quantum critical points where the entropy usually vanishes at $T = 0$, but features an unconventional power law, $S(T) \propto T^x$.

For the models at hand, the impurity contribution to the low-temperature entropy is obtained by a perturbative evaluation of the thermodynamic potential and taking the temperature derivative. In the present expansion the result has the form $S_{\text{imp}}(T = 0) = \ln(2S + 1) + \Delta S_{\text{imp}}$ with $S = \frac{1}{2}$.

It is worth emphasizing that the aim of the ϵ expansion for the entropy is not to capture *singular* corrections (as is the case for observables which develop anomalous power laws), but to determine the power series for the coefficient of an observable with *regular* behavior. As shown below, fully universal quantities can be obtained by correctly interpreting the result of the perturbative calculation. The situation is similar to the evaluation of the impurity susceptibility in Sec. IV, where the coefficient C_{imp} in Eq. (35) was obtained in an expansion in ϵ and r .

The diagrams necessary for the evaluation of the thermodynamic potential are shown in Fig. 3. In the following we list the corresponding results; some details of the evaluation are described in App. C – in particular it is important to note that certain *disconnected* diagrams appear in the expansion of the thermodynamic potential.

The coupling to the fermions, Fig. 3b1, yields

$$\Delta S_{\text{imp}}^{(f)} = \frac{3j_0^2}{8} \frac{1}{4T^2} \int dk_1 dk_2 \frac{|k_1|^r |k_2|^r}{k_1 - k_2} \frac{k_2}{\cosh^2(k_2/2T)}.$$

The integrals can be performed in the limit of infinite UV cutoff, with the result

$$\Delta S_{\text{imp}}^{(f)} = \frac{3\pi}{8} j_0^2 T^{2r} \tan \frac{\pi r}{2} (2 - 2^{1-2r}) \Gamma(2 + 2r) \zeta(1 + 2r)$$

where $\Gamma(z)$ and $\zeta(z)$ are the Gamma and Riemann Zeta functions. In the weak-coupling regime the above term goes to zero as T^{2r} for $T \rightarrow 0$, thus the entropy at the LM fixed point is $\ln 2$. However, in the quantum critical

region, the dimensionless combination $j_0 T^r$ approaches a universal value at the F-CR fixed point, and a universal correction to the impurity entropy arises. This is easily seen by replacing j_0 with the renormalized coupling j , defined by $j_0 = j \mu^{-r}$. Using $(T/\mu)^r = 1 + r \ln(T/\mu) + \mathcal{O}(r^2)$ and expanding in r one finally obtains:

$$\Delta S_{\text{imp}}^{(f)} = \frac{3\pi^2 \ln 2}{8} j^2 r. \quad (40)$$

Notably, this j^2 correction to S_{imp} is suppressed by an additional factor of r . We have verified that the contributions from the next-order diagram, Fig. 3b2, proportional to j^3 , also receive an additional factor of r ; thus the term (40) is the only one to order r^3 at the F-CR fixed point.

The lowest-order bosonic contribution from Fig. 3c1 turns out to vanish identically for the $g = 0$ case, i.e., for non-interacting bosons, because the contribution of this diagram to the thermodynamic potential is temperature-independent. For interacting bosons, we take into account the T -dependent mass renormalization arising from g , and obtain using (7) in a similar manner as above:

$$\Delta S_{\text{imp}}^{(b2, \text{int})} = -\frac{3\pi^2}{8} \gamma^2 \sqrt{\frac{10\epsilon}{33}}. \quad (41)$$

For non-interacting bosons, non-vanishing corrections to the entropy arise only at order γ^4 from the diagrams shown in Figs. 3c2, 3c3. With Eq. (C4) one finds:

$$\begin{aligned} \Delta S_{\text{imp}}^{(b4)} &= -\partial_T \left((3c2) + (3c3) - (3c1)^2 \right) \\ &= -\frac{3\pi^2}{8} \gamma^4. \end{aligned} \quad (42)$$

With these perturbative results, we can finally evaluate the residual impurity entropy at the intermediate-coupling fixed points, to the order available.

$$\text{F-CR} : S_{\text{imp}} = \ln 2 \left(1 + \frac{3\pi^2}{8} r^3 \right) + \mathcal{O}(r^5),$$

$$\text{FB-CR} : S_{\text{imp}} = \ln 2 - \frac{3\pi^2}{16} \sqrt{\frac{10}{33}} \epsilon^{3/2} + \mathcal{O}(\epsilon, r)^2,$$

$$\text{B-FL} : S_{\text{imp}} = \ln 2 - \frac{3\pi^2}{16} \sqrt{\frac{10}{33}} \epsilon^{3/2} + \mathcal{O}(\epsilon^2). \quad (43)$$

The last two lines are for interacting bosons³⁶. In principle, the two-loop result for the impurity entropy can be obtained from the diagrams in Fig. 3 using the methods of Ref. 23; we do not attempt this here. The entropies for the FB-CR and B-FL fixed points get modified for non-interacting bosons ($g = 0$):

$$\text{FB-CR} : S_{\text{imp}} = \ln 2 - \frac{3\pi^2}{32} \epsilon^2 + \mathcal{O}(\epsilon^3, r^3),$$

$$\text{B-FL} : S_{\text{imp}} = \ln 2 - \frac{3\pi^2}{32} \epsilon^2 + \mathcal{O}(\epsilon^3). \quad (44)$$

In App. D we present a large- N calculation¹⁹ of the entropy at the B-FL fixed point, which also yields an answer

of the form $S_{\text{imp}} = \ln 2 - \mathcal{O}(\epsilon^2)$ for small ϵ , but provides results³⁷ for all $0 \leq \epsilon \leq 2$.

All of the above expressions are consistent with

$$\begin{aligned} S_{\text{imp}}^{\text{F-CR}} &\geq \ln 2 \geq S_{\text{imp}}^{\text{B-FL}}, \\ S_{\text{imp}}^{\text{F-CR}} &\geq S_{\text{imp}}^{\text{FB-CR}} \geq S_{\text{imp}}^{\text{B-FL}}; \end{aligned} \quad (45)$$

these are the conditions that the impurity entropy always decreases in the course of the renormalization group flow³³. Apparently, in the ϵ expansion we have $S_{\text{imp}}^{\text{FB-CR}} = S_{\text{imp}}^{\text{B-FL}}$ to the order calculated here, because the coupling constants γ of both fixed points are equal to one-loop order. However, it can be expected that in general $S_{\text{imp}}^{\text{FB-CR}} > S_{\text{imp}}^{\text{B-FL}}$ due to the facts that $\gamma^{\text{FB-CR}} < \gamma^{\text{B-FL}}$ and $\Delta S_{\text{imp}}^{(f)} > 0$.

For the F-CR fixed point, the NRG calculations of Ref. 11 indicated a very small deviation of the impurity entropy from $\ln 2$. We have repeated these calculations and have found indications for a correction which scales as r^3 at small r , however, the accuracy is not sufficient to reliably determine the prefactor. Note that the entropy of the fermionic particle-hole symmetric critical fixed point also approaches¹¹ the value of $\ln 2$ for $r \rightarrow \frac{1}{2}$, rendering the corrections to $\ln 2$ tiny for all $0 < r < \frac{1}{2}$. Interestingly, a similar entropy calculation can be done for the particle-hole *asymmetric* critical fixed point of the pseudogap Kondo model, where the expansion is performed around the upper-critical “dimension” $r = 1$. The corresponding result¹³ is $S_{\text{imp}} = \ln 3 - (8/9)(1-r)\ln 2$, in good agreement with numerics¹¹.

VI. T MATRIX

An important quantity in a Kondo model is the conduction electron T matrix, describing the scattering of the c electrons off the impurity. It is useful to define a propagator, G_T , of the composite operator $T_\sigma = f_\sigma^\dagger f_{\sigma'} c_{\sigma'}$, such that the T matrix is given by $T(\omega) = j_0^2 G_T(\omega)$. As with the local susceptibility, we expect a power law behavior of the T matrix spectral density at the intermediate-coupling fixed points:

$$T(\omega) \propto \frac{1}{\omega^{-r-\eta_T}}, \quad (46)$$

note that at tree level $G_T \propto \omega^r$ in the present pseudogap problem.

We now evaluate the lowest-order diagrams of the T propagator in an expansion in γ and j , introduce a G_T renormalization factor, Z_T , and determine Z_T by minimal subtraction of poles. The result, given in (A15), yields the anomalous exponent as $\eta_T = -2j + j^2 + 2(\gamma^2 - \gamma^4)$. Evaluating this at the RG fixed points we obtain

$$\begin{aligned} \text{F-CR} : \quad \eta_T &= -2r, \\ \text{FB-CR} : \quad \eta_T &= -2r, \\ \text{B-FL} : \quad \eta_T &= \begin{cases} \epsilon - \epsilon^2 \left(\frac{5}{242} + \frac{5\pi^2}{66} \right) + \mathcal{O}(\epsilon^3) & (g_0 \neq 0) \\ \epsilon & (g_0 = 0) \end{cases}. \end{aligned} \quad (47)$$

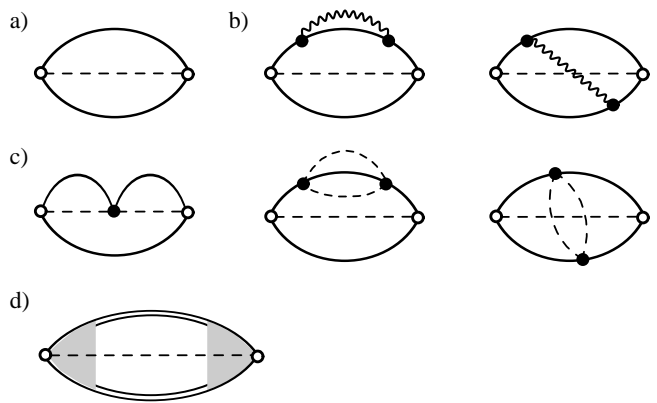


FIG. 4: Feynman diagrams for the Green’s function G_T entering the conduction electron T matrix. Notation is as in Fig. 3; the double line is the full f propagator, the shaded area the full j vertex, and the open dots are the external sources. a) Bare T matrix. b) and c) Corrections from the fermionic and bosonic baths. d) Full T matrix.

Remarkably, the two-loop corrections for F-CR and FB-CR have cancelled. As announced in Ref. 20, this cancellation holds to all orders. The argument parallels the one for anomalous exponent of the local susceptibility of *non-interacting* bosons, given in Refs. 5,18. For fermions *without* a relevant self-interaction, all diagrams for G_T can be obtained from the first diagram with *full* j vertices and *full* f electron propagators. This gives the relation $Z_T^{-1} = Z_j^2/Z_f^2$; note that the corresponding relation for the local susceptibility of non-interacting bosons is $Z_\chi^{-1} = \tilde{Z}_\gamma^2/Z_f^2$. Using the definition of Z_j (A5) and taking the derivative w.r.t. $(\ln \mu)$ at fixed bare j_0 , we obtain $0 = -r + \beta(j)/j - \eta_T/2$. Thus, at any RG fixed point with finite j^* we find the exact result

$$\eta_T = -2r \Rightarrow T(\omega) \propto \omega^{-r} \quad (48)$$

which applies to the F-CR and FB-CR fixed points. For F-CR it is in perfect agreement with NRG results^{10,38}.

At finite temperatures, hyperscaling again implies a scaling form of the T matrix, which can be written as:

$$T(\omega, T) = \frac{\mathcal{B}_T}{\omega^r} \Phi_T\left(\frac{\omega}{T}\right), \quad (49)$$

valid at both the F-CR and FB-CR fixed points.

Away from criticality, scaling is also obeyed as function of the distance from the critical point, similar to Eq. (32). We note that in the LM regime, bare perturbation theory is applicable and gives $T(\omega) \propto \omega^r$. Then, for $j_0 \lesssim j_{0c}$ in the pseudogap Kondo problem, one finds a crossover from $T(\omega) \propto \omega^{-r}$ for $\omega \gg T^*$ to $T(\omega) \propto \omega^r$ for $\omega \ll T^*$, in agreement with NRG results¹⁰.

For transport experiments in a pseudogap system with dilute magnetic impurities, we can estimate the impurity-induced resistivity ρ_{imp} by evaluating the conduction electron bubble with the lowest-order self energy. The

above implies a divergence $\rho_{\text{imp}} \propto T^{-r(1-r)}$ at criticality (with logarithmic corrections at both $r = 0$ and $r = 1$), whereas ρ_{imp} vanishes according to $\rho_{\text{imp}} \propto T^{r(1-r)}$ away from criticality. Here, the $(1-r)$ factor in the exponent arises from the momentum integration (consistent with a resistivity being independent of the scattering rate at $r = 1$, Ref. 39). Thus, for $0 < r < 1$ and sufficiently close to the critical point, one expects a characteristic peak in the temperature dependence of ρ_{imp} , located at the crossover temperature T^* .

VII. DYNAMICAL MEAN-FIELD THEORY

Magnetic ordering transitions in certain heavy-fermion compounds, like $\text{CeCu}_{6-x}\text{Au}_x$ and YbRh_2Si_2 , have been proposed to be accompanied by the breakdown of Kondo screening at criticality^{6,40}. One particular scenario⁶ employs an extended DMFT description for this transition, where the original Kondo lattice model is mapped onto a self-consistent version of the Fermi-Bose Kondo model, and the critical point of the bulk system is mapped onto the BF-CR critical point of the impurity model. Recent numerical calculations have found the existence of such a transition in the extended DMFT for an anisotropic Kondo lattice model⁴¹ (however, competing claims have also been published⁴²).

In the following, we want to focus on a property of such a locally-critical point which has not received much attention so far, namely the entropy and specific heat near the critical point. In principle, our statements will apply to all quantum critical points in DMFT where the effective impurity model is itself critical at the bulk transition. (Note that this does *not* seem to be the case for the much-studied Mott metal-insulator transition in the one-band Hubbard model¹.)

To be specific, let us consider the thermodynamic potential of an Anderson lattice model, treated within extended DMFT (equations for a $t - J$ model are similar). It has been shown in Ref. 43 that the lattice potential (per site) can be written as the sum of impurity and bath contributions,

$$\begin{aligned} \Omega &= \Omega_{\text{imp}} + \Omega_c + \Omega_\phi, \\ \Omega_c &= T \sum_{\omega_n} \frac{1}{N_s} \sum_k \ln[G_c(k, i\omega_n)/G_{\text{loc}}(i\omega_n)] e^{i\omega_n 0^+}, \\ \Omega_\phi &= \frac{T}{2} \sum_{\nu_n} \frac{1}{N_s} \sum_k \ln[D_\phi(k, i\nu_n)/\chi_{\text{loc}}(i\nu_n)] e^{i\nu_n 0^+}, \end{aligned} \quad (50)$$

where $G_c(k, i\omega_n)$ and $D_\phi(k, i\nu_n)$ are the fermionic and bosonic bath Green's functions, respectively, and N_s is the number of lattice sites. G_{loc} and χ_{loc} are the (local) impurity electron propagator and susceptibility – in our notation, G_{loc} is the propagator of the f fermions. The lattice entropy (per site) is simply $-\partial_T \Omega$. The temperature derivatives of the two terms Ω_c and Ω_ϕ vanish in the zero-temperature limit: note that they just represent

contributions from systems of free fermions or bosons, where the respective densities of states are (at most) logarithmically singular within the locally-critical point scenario in two space dimensions⁶.

Thus, the entropy of the impurity model, $-\partial_T \Omega_{\text{imp}}$, is the only contribution to the total entropy of the lattice model which survives as $T \rightarrow 0$. The results of Sec. V suggest that the critical point of the Fermi-Bose Kondo model, BF-CR, generically has a finite residual entropy³⁷, with the perturbative result given in Eqs. (43,44). According to (50), this implies an extensive entropy of the Kondo lattice model described by extended DMFT, which should be present at the $T = 0$ critical point as well as in the low-temperature limit of the quantum critical region. As the ground state entropies of the stable phases (heavy Fermi liquid and antiferromagnet for the case of the Kondo lattice) are non-extensive, a huge anomaly in the specific heat, $C = T(\partial S/\partial T)$, should be observed upon crossing the phase diagram at low temperatures above the quantum critical point. To our knowledge, this has not been observed experimentally. Furthermore, it can be considered unlikely that a quantum critical point of a lattice model displays an extensive residual entropy, as such a point would be unstable to any perturbation. (Note that a generic lattice quantum critical point has only *one* unstable direction in the RG flow, and vanishing residual entropy.)

Finally, as detailed in Ref. 20, the DMFT self-consistency equation for the fermionic bath at local criticality can only be fulfilled with a fermionic spectrum with $r = 0$. Therefore, the local critical point displays at most logarithmic corrections to a metallic local density of states, and one can thus expect a logarithmic T -dependence of the resistivity. A discussion of the resistivity away from criticality requires to consider the fully self-consistent problem, and is beyond the scope of this paper.

VIII. DISCUSSION AND CONCLUSIONS

We have calculated critical properties of a Fermi-Bose Kondo model, describing an impurity spin coupled to both fermionic quasiparticles with a pseudogap DOS and collective mode bosons, using renormalization group techniques. In particular, we have determined the impurity susceptibilities and residual entropies at different intermediate-coupling fixed points.

Our results for the phase transition in the pseudogap Kondo model can be compared with numerical results obtained by high-accuracy NRG calculations. The excellent agreement strongly suggests that the renormalized perturbation expansion approach for critical properties is reliable in the context of impurity quantum phase transitions (provided that the fixed point is in the applicability range of the renormalization group procedure), and gives numerically accurate results for a *finite* range of the (small) parameters r, ϵ .

Remarkably, the physics found in the present models is somewhat different from the one of the two-channel Kondo effect. In the two-channel problem, a number of thermodynamic properties vanish in the strict scaling limit, and corrections to scaling yield the leading low-temperature observables. In contrast, for the intermediate-coupling fixed points considered here, the predictions of naive scaling apply. The reason for this difference apparently is the finite tree-level scaling dimension of the impurity couplings in the present models, whereas the coupling in the metallic two-channel problem is marginal.

As can be seen from the perturbative results presented in this paper, the prefactors of most of the higher-order corrections in the ϵ expansion of physical quantities are not small, and thus no quantitatively accurate numbers can be obtained for $\epsilon = 1$. It may be possible to use certain resummation techniques of the perturbative expansion – this is beyond the scope of this work. Nevertheless, we expect that the qualitative physics is captured by the present study, which is supported by the large- N calculations in Ref. 19 and App. D for the purely bosonic Kondo problem.

On the single-impurity application side, the models discussed here can describe magnetic impurities in strongly correlated materials, where the interplay of quasiparticles and collective low-energy excitations is a central ingredient. As has been argued elsewhere^{20,38,44}, the pseudogap Kondo model appears relevant for impurity moments in high-temperature superconductors. Detailed calculations of the local density of states in the vicinity of the impurity^{38,44} have been compared with scanning tunneling microscopy results⁴⁵ in Zn-doped $\text{Bi}_2\text{Sr}_2\text{CaCu}_2\text{O}_{8+\delta}$. In addition, the interplay with bulk spin fluctuations possibly explains the large doping dependence of the Kondo temperature across the phase diagram of $\text{YBa}_2\text{Cu}_3\text{O}_{7-\delta}$ ^{14,15}, as has been explicitly demonstrated in calculations using the pseudogap Fermi-Bose Kondo model in Ref. 20. In this case, the inclusion of the bosonic self-interaction is important, as fermionic quasiparticles and spin fluctuations are decoupled in the low-energy physics of a d -wave superconductor, and Landau damping is absent¹⁹.

Finally we have discussed the issue of the ground-state entropy in scenarios of local quantum criticality, described by dynamical mean-field theory. We found that the finite residual entropy of the critical impurity model, found in Sec. V³⁷, leads to an extensive ground-state entropy of the lattice model, which appears unlikely to be realized in a finite-dimensional system. One can conclude that the dynamics at a heavy-fermion critical point, which is associated with the breakdown of Kondo screening, *cannot* be entirely local, as described by dynamical mean-field approaches. In other words, at lowest temperatures the entropy has to be quenched by non-local correlations. Versions of DMFT can still provide a reasonable description of the physics at intermediate energies and temperatures.

Acknowledgments

We thank R. Bulla, L. Fritz, A. Polkovnikov, and S. Sachdev for discussions and collaborations on related work, as well as P. Coleman, S. Florens, O. Parcollet, A. Rosch, and Q. Si for helpful discussions. MV is particularly grateful to C. Lorenz for exposing the role of Eq. (B1). This research was supported by the DFG through the Center for Functional Nanostructures Karlsruhe.

APPENDIX A: FIELD-THEORETIC RG TO TWO LOOPS

The renormalization group to two-loop order is conveniently done in the field-theoretic scheme, employing dimensional regularization and minimal subtraction of poles. Using the conventions of Ref. 29, we introduce renormalized fields and dimensionless couplings for the bulk bosons

$$\phi_\alpha = \sqrt{Z} \phi_{R\alpha}, \quad (\text{A1})$$

$$g_0 = \frac{\mu^\epsilon Z_4}{Z^2 S_{d+1}} g \quad (\text{A2})$$

and for the impurity

$$f_\sigma = \sqrt{Z_f} f_{R\sigma}, \quad (\text{A3})$$

$$\gamma_0 = \frac{\mu^{\epsilon/2} \tilde{Z}_\gamma}{Z_f \sqrt{Z \tilde{S}_{d+1}}} \gamma, \quad (\text{A4})$$

$$j_0 = \frac{\mu^{-r} Z_j}{Z_f} j; \quad (\text{A5})$$

here μ is a renormalization energy scale, and

$$S_d = \frac{2}{\Gamma(d/2)(4\pi)^{d/2}},$$

$$\tilde{S}_d = \frac{\Gamma(d/2 - 1)}{4\pi^{d/2}}. \quad (\text{A6})$$

No renormalizations are needed for the fermions as their self-interaction is assumed to be irrelevant in the RG sense.

The needed diagrams have been evaluated in Refs. 5 and 21 and will not be repeated here. Minimal subtraction of poles yields the renormalization factors for the bulk bosons²⁹

$$Z = 1 - \frac{5g^2}{144\epsilon},$$

$$Z_4 = 1 + \frac{11g}{6\epsilon} + \left(\frac{121}{36\epsilon^2} - \frac{37}{36\epsilon} \right) g^2 \quad (\text{A7})$$

and for the impurity

$$Z_f = 1 + \frac{3j^2}{16r} - \frac{3\gamma^2}{4\epsilon} + \left(-\frac{15}{32\epsilon^2} + \frac{3}{8\epsilon} \right) \gamma^4,$$

$$\begin{aligned}\tilde{Z}_\gamma &= 1 - \frac{j^2}{16r} + \frac{\gamma^2}{4\epsilon} + \left(\frac{9}{32\epsilon^2} - \frac{1}{8\epsilon}\right)\gamma^4 + \frac{5g\pi^2\gamma^2}{72\epsilon}, \\ Z_j &= 1 + \frac{j}{r} + \left(\frac{1}{r^2} - \frac{1}{16r}\right)j^2 + \frac{\gamma^2}{4\epsilon} + \left(\frac{9}{32\epsilon^2} - \frac{1}{8\epsilon}\right)\gamma^4 \\ &\quad + \left(\frac{1}{4\epsilon} + \frac{1}{\epsilon - r}\right)\frac{j\gamma^2}{r}.\end{aligned}\quad (\text{A8})$$

The RG beta functions can now be evaluated by taking the μ derivatives of (A2), (A4), and (A5) at fixed values of bare coupling constants. For the bulk coupling we find the known result:

$$\beta(g) \equiv \mu \frac{dg}{d\mu} \Big|_{g_0} = -\epsilon g + \frac{11g^2}{6} - \frac{23g^3}{12} \quad (\text{A9})$$

which has the stable fixed point

$$g^* = \frac{6\epsilon}{11} + \frac{414\epsilon^2}{1331}. \quad (\text{A10})$$

The impurity couplings are governed by the following beta functions:

$$\begin{aligned}\beta(\gamma) &= -\frac{\epsilon\gamma}{2} + \gamma^3 - \gamma^5 + \frac{5g^2\gamma}{144} + \frac{5\pi^2g\gamma^3}{36} + \frac{j^2\gamma}{2}, \\ \beta(j) &= rj - j^2 + \frac{j^3}{2} + j\gamma^2 - j\gamma^4.\end{aligned}\quad (\text{A11})$$

Using these beta functions one obtains the fixed point values of the couplings quoted in Sec. III B.

The anomalous field dimension η_f is obtained from

$$\eta_f = \mu \frac{d \ln Z_f}{d\mu} \Big|_{g^*, \gamma^*, j^*}, \quad (\text{A12})$$

where the derivative is evaluated at the RG fixed point.

To calculate the anomalous exponent of the local susceptibility, a renormalization factor, Z_χ , for the two-point correlations of the impurity spin has to be introduced. The required diagrams have been evaluated in Refs. 5 and 19; the result for Z_χ within the minimal subtraction scheme is

$$Z_\chi = 1 - \frac{2\gamma^2}{\epsilon} + \frac{\gamma^4}{\epsilon} + \frac{j^2}{2r}. \quad (\text{A13})$$

Employing

$$\eta_\chi = \mu \frac{d \ln Z_\chi}{d\mu} \Big|_{g^*, \gamma^*, j^*} \quad (\text{A14})$$

one obtains the η_χ values quoted in Sec. IV.

Similarly, the renormalization factor for the T matrix, discussed in Sec. VI, is obtained as

$$\begin{aligned}Z_T &= 1 - \frac{2j}{r} + \frac{j^2}{2r} + \frac{j^2}{r^2} - \frac{2\gamma^2}{\epsilon} + \frac{\gamma^4}{\epsilon} \\ &\quad + \left(\frac{4}{\epsilon} - \frac{2}{r}\right)\frac{j\gamma^2}{r - \epsilon}.\end{aligned}\quad (\text{A15})$$

APPENDIX B: ROLE OF $\langle \hat{Q} \rangle$

Here we briefly discuss the role of the denominator appearing in the equation for observables, (8), within the pseudo-fermion technique employed here. (Note that a similar denominator also appears in the formalism used in Ref. 19.)

For a renormalization group procedure which directly calculates renormalizations of vertices and propagators (as the momentum shell method), the denominator does formally not appear. In contrast, when calculating true observables, as e.g. done in Ref. 19, $\langle \hat{Q} \rangle$ needs to be taken into account. Importantly, approximating the denominator with its leading contribution, $2 \exp(-\beta\lambda)$, is in general not sufficient, as the denominator contains – as the numerator of (8) – contributions from all orders in an expansion in the non-linear couplings.

However, in the calculation of critical exponents using, e.g., the minimal subtraction scheme, one only needs to keep track of contributions which develop poles in ϵ after dimensional regularization, i.e., are logarithmic at the marginal dimension. Typically, the denominator does *not* develop such poles, which can be seen by comparing power counting for response functions, i.e., second derivatives of the thermodynamic potential, and for the potential itself. Therefore, for the calculation of anomalous exponents it is permissible to ignore the perturbation expansion of $\langle \hat{Q} \rangle$, as done in Ref. 5.

In contrast, when calculating a quantity which does *not* develop an anomalous power law, like χ_{imp} in the present impurity problems, all poles cancel, and one has to collect contributions non-singular in ϵ . Those also arise from a perturbative expansion of the denominator, and typically cancel corresponding terms from the numerator. Explicitly, we have to lowest order:

$$\langle \hat{Q} \rangle = 2 \exp(-\lambda\beta) \left(1 - \frac{3}{8T} \gamma_0^2 \int \frac{d^d k}{(2\pi)^d} \frac{1}{\epsilon_k^2} \right); \quad (\text{B1})$$

to this order only the bosonic part enters, and ϵ_k is the boson dispersion appearing in $D_\phi(k, \omega_n) = (\omega_n^2 + \epsilon_k^2)^{-1}$.

Finally, we note that in certain impurity problems the real part of the propagator renormalization requires the introduction of a suitable counter-term – physically this reflects the shift of the phase transition point, arising from the real part of a self-energy. In the present case no counter-terms are necessary.

APPENDIX C: PERTURBATIVE EXPANSION FOR THE IMPURITY ENTROPY

In this appendix we describe the perturbation theory for the impurity part of the thermodynamic potential. The impurity spin is represented by f pseudo-fermions as above, together with the chemical potential in the limit $\lambda \rightarrow \infty$. We shall illustrate that the correct treatment of this limit has non-trivial consequences for the higher-order diagrammatic expansion of the entropy.

The starting point is the partition function in the physical sector of the Hilbert space ($\hat{Q} = f_\nu^\dagger f_\nu = 1$), which can be written as

$$\frac{Z_{\text{imp}}}{Z_{\text{imp},0}} = \lim_{\lambda \rightarrow \infty} \frac{\langle \hat{Q} \rangle_\lambda}{\langle \hat{Q} \rangle_{\lambda,0}} \quad (\text{C1})$$

Here, $\langle \dots \rangle_\lambda$ is an expectation value with the full Hamiltonian in the presence of λ as above, and $\langle \dots \rangle_{\lambda,0}$ is the expectation value in the absence of the coupling between impurity and baths. The above expression is easily understood: for $\lambda \rightarrow \infty$, $\langle \hat{Q} \rangle_\lambda$ is the partition in the physical sector times $\exp(-\lambda\beta)$, i.e., the ‘‘factor’’ \hat{Q} suppresses the $\hat{Q} = 0$ part of the Hilbert space. Further, in this limit $\langle \hat{Q} \rangle_{\lambda,0} = 2 \exp(-\lambda\beta)$, and the unperturbed impurity part of the partition function is just $Z_{\text{imp},0} = 2$ for a spin- $\frac{1}{2}$ impurity. Importantly, the limit $\lambda \rightarrow \infty$ in Z_{imp} suppresses the contributions from disconnected diagrams, consisting of more than one loop of f pseudo-fermions, because those are smaller by further powers of $\exp(-\lambda\beta)$.

The thermodynamic potential is given by

$$\Omega_{\text{imp}} - \Omega_{\text{imp},0} = -T \ln \frac{Z_{\text{imp}}}{Z_{\text{imp},0}}. \quad (\text{C2})$$

The partition function (C1) can now be expanded in the impurity couplings using standard diagrammatics, and then the log in (C2) is expanded to the required order. There is now *no* cancellation of disconnected diagrams in Ω_{imp} , because those diagrams do not appear in Z_{imp} – this reflects the fact that we are not expanding around a system of free particles here.

For the bosonic impurity problem, we have

$$\frac{Z_{\text{imp}}}{Z_{\text{imp},0}} = 1 + \frac{\gamma_0^2}{2} D^{(2)} + \frac{\gamma_0^4}{4} D^{(4)} + \dots \quad (\text{C3})$$

where $D^{(n)}$ is the sum of all n -th order different *connected* diagrams; $D^{(2)}$ and $D^{(4)}$ are shown in Fig. 3c. Thus,

$$\frac{\Omega_{\text{imp}} - \Omega_{\text{imp},0}}{-T} = \frac{\gamma_0^2}{2} D^{(2)} + \frac{\gamma_0^4}{4} D^{(4)} - \frac{\gamma_0^4}{8} D^{(2)^2} + \dots, \quad (\text{C4})$$

i.e., the expansion for the thermodynamic potential contains disconnected diagrams!

The entropy is obtained from Ω_{imp} by $S_{\text{imp}} = -\partial_T \Omega_{\text{imp}}$. Power counting shows that $S_{\text{imp}} = \ln 2$ as $T \rightarrow 0$ in the cases where the fixed point value of the impurity coupling is zero (as is the case, e.g., in the Bose-Kondo model for $d > 3$ space dimensions). Then, only subleading corrections arise from the coupling to the bath. In contrast, in the case of a finite renormalized coupling j^* or γ^* , bare perturbation theory is infrared divergent, as for standard problems below their upper-critical dimension. Proceeding in the scheme of renormalized perturbation theory, the perturbative result (to lowest non-trivial order) can be expressed in terms of the renormalized couplings. At the RG fixed point, the couplings can then be replaced by their fixed-point values, and the result for the entropy is finite as $T \rightarrow 0$.

The impurity part of the thermodynamic potential diverges with the cutoff, i.e., we have $\Omega_{\text{imp}} = E_{\text{imp}} - T S_{\text{imp}}$, where E_{imp} is the non-universal (cutoff-dependent) impurity contribution to the ground-state energy. However, the impurity entropy S_{imp} is fully universal, and the UV cutoff can be sent to infinity *after* taking the temperature derivative of Ω_{imp} .

APPENDIX D: LARGE- N THEORY OF THE BOSE KONDO PROBLEM – ENTROPY

As the perturbative method employed in the body of the paper is restricted to small $\epsilon = 3 - d$, alternative approaches are desirable which can provide results for all ϵ . In Ref. 19 a dynamic large- N approach to the bosonic Kondo problem has been developed. Here we shall use this approach to evaluate the impurity entropy at the B-FL fixed point in arbitrary space dimension d , which complements the results of Sec. V.

We begin by summarizing the large- N theory of Ref. 19. The impurity spin symmetry is generalized from SU(2) to SU(N). The spin operator is represented by auxiliary fermions f_ν ($\nu = 1, \dots, N$), and a chemical potential λ_0 is introduced to enforce the constraint $f_\nu^\dagger f_\nu = Nq_0$. We will restrict the considerations to $q_0 = 1/2$; this choice has the advantage of preserving particle-hole symmetry, such that the chemical potential λ_0 is actually zero for all temperatures. The Hamiltonian is given by the natural large- N generalization of $\mathcal{H}_{\text{imp}} + \mathcal{H}_\phi$ of Sec. II, where the ϕ field now has $N^2 - 1$ components; for details see Ref. 19. Taking the limit $N \rightarrow \infty$ results in a dynamic saddle point⁴⁶, and the impurity physics is captured by a self-consistent integral equation,

$$\Sigma_f(\tau) = -\gamma_0^2 D_\phi(\tau) G_f(\tau), \quad (\text{D1})$$

where D_ϕ is the local spin fluctuation propagator (6), and the self-energy Σ_f is defined by:

$$G_f^{-1}(i\omega_n) = i\omega_n - \lambda_0 - \Sigma_f(i\omega_n). \quad (\text{D2})$$

Here $G_f(\tau) = -\langle T f(\tau) f^\dagger(0) \rangle$ is the *full* auxiliary fermion Green’s function in standard notation. Clearly, (D1) represents a summation of all self-energy diagrams with non-crossing boson lines, somewhat similar to the non-crossing approximation known from fermionic Kondo physics^{2,46}. In writing down the above equations we have assumed full SU(N) symmetry and dropped the corresponding SU(N) indices. Finally, λ_0 is determined by the constraint equation:

$$G_f(\tau = 0^-) = \frac{1}{\beta} \sum_n G_f(i\omega_n) e^{i\omega_n 0^+} = Nq_0, \quad q_0 = \frac{1}{2}$$

which is designed to satisfy the constraint $f_\nu^\dagger f_\nu = Nq_0$ on average.

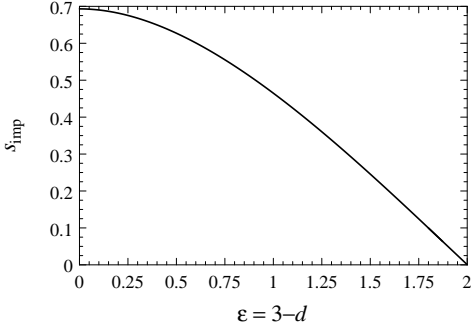


FIG. 5: Large- N result (D10) for the residual impurity entropy (per flavor) at the B-FL fixed point, valid for a bath of non-interacting bosons in $(3 - \epsilon)$ space dimensions.

In the following we concentrate on the bulk critical point, $s = s_c$, where the bosonic spectrum is gapless, $\rho_\phi(\omega) \propto \text{sgn}(\omega)|\omega|^{1-\epsilon}$. It has been established in Ref. 19 that the $T = 0$ result for the fermionic Green's function obeys:

$$G_f(\tau) \sim \frac{1}{\tau^{\epsilon/2}}, \quad \rho_f(\omega) \sim |\omega|^{\epsilon/2-1}. \quad (\text{D3})$$

in the long-time or low-energy limit; here $\rho_f(\omega)$ is the spectral density of G_f . For the case of non-interacting bosons it is possible to obtain an analytical result for the finite-temperature scaling form of G_f ,

$$G_f(\tau) = -A \frac{T^{\epsilon/2}}{\gamma_0^\epsilon} \left(\frac{\pi}{\sin \pi(\tau T)} \right)^{\epsilon/2}, \quad (\text{D4})$$

which is dictated by conformal invariance⁴⁶; A is an amplitude prefactor depending on ϵ .

The local susceptibility in the large- N limit,

$$\chi_{\text{loc}} = - \int_0^\beta d\tau G_f(\tau) G_f(-\tau), \quad (\text{D5})$$

can be evaluated directly at the critical point, $s = s_c$, with the result $\chi_{\text{loc}} \propto T^{-1+\epsilon}$. Thus we have the large- N result

$$\eta_\chi = \epsilon, \quad (\text{D6})$$

which coincides with the exact result (29) for non-interacting bosons in the $\text{SU}(2)$ -symmetric Bose Kondo problem.

Now we proceed with the calculation of the residual impurity entropy, following the method by Parcollet *et al.*⁴⁶ for the fermionic NCA. At the saddle point, the impurity part of the free energy per flavor can be written as:

$$f_{\text{imp}} = q_0 \lambda_0 + T \sum_n \ln G_f(i\omega_n) - \int_0^\beta d\tau \Sigma_f(\tau) G_f(-\tau). \quad (\text{D7})$$

For particle-hole symmetry, $q_0 = 1/2$, we have $\lambda_0 = 0$. Furthermore, the last term in (D7) behaves as $\text{const} + \mathcal{O}(T^{1+\epsilon/2})$, and thus does not contribute to the zero-temperature entropy. It remains to evaluate the contribution from $\text{Tr} \ln G_f$. As shown in Ref. 46, it can be written as:

$$f_{\text{imp}} = \frac{1}{\pi} \int_{-\infty}^{\infty} d\omega n_f(\omega) \left[\arctan \left(\frac{G'_f(\omega)}{G''_f(\omega)} \right) - \frac{\pi}{2} \right], \quad (\text{D8})$$

with G'_f, G''_f being the real and imaginary part of the finite-temperature retarded fermion Green's function, and n_f is the Fermi factor.

In the following we restrict our attention to the case of non-interacting bosons which allows to make analytical progress. The temperature derivative of the above expression has to be taken using the scaling form (D4) of G_f . After straightforward algebra in analogy to Sec. VI of Ref. 46 we find for the impurity entropy (per flavor):

$$s_{\text{imp}} = -\frac{2}{\pi} \int_0^1 \frac{du}{1-u^2} [u \arctan(ut) - \arctan t], \quad (\text{D9})$$

where the substitutions $1/t = \tan(\pi\epsilon/4)$ and $u = \tanh(\omega/2T)$ have been employed. The above result can be re-written as

$$s_{\text{imp}} = \ln 2 - \frac{2}{\pi} \int_0^{1/t} dv \frac{v \arctan(1/v)}{1+v^2}. \quad (\text{D10})$$

This represents our large- N result for the impurity entropy at the B-FL fixed point for non-interacting bosons. Numerical evaluation of the integral yields s_{imp} as shown in Fig. 5. For small ϵ , where $1/t = \pi\epsilon/4$, the correction to the $\log 2$ entropy is quadratic in ϵ , which is similar to the $\text{SU}(2)$ result in (44). In particular, we see that s_{imp} is *finite* for all $0 \leq \epsilon < 2$, with the numerical value

$$s_{\text{imp}}(d=2) = 0.4648477 \quad (\text{D11})$$

at $\epsilon = 1$. (Note that, e.g., the local susceptibility is only singular for $0 \leq \epsilon \leq 1$.) s_{imp} vanishes as $d \rightarrow 1$, i.e., at the lower critical dimension of the bulk theory, where G_f is no longer singular – this is consistent with the considerations of Ref. 28.

Unfortunately, the present large- N theory cannot be easily generalized to the Fermi-Bose Kondo model with a single fermionic screening channel. Instead, the natural dynamic large- N formulation of the fermionic sector leads to a multichannel Kondo model⁴⁶, which, however, does not display a strong-coupling fixed point with vanishing residual entropy.

-
- ¹ W. Metzner and D. Vollhardt, Phys. Rev. Lett. **62**, 324 (1989); A. Georges, G. Kotliar, W. Krauth, and M. J. Rozenberg, Rev. Mod. Phys. **68**, 13 (1996).
- ² A. C. Hewson, *The Kondo Problem to Heavy Fermions*, Cambridge University Press, Cambridge (1997).
- ³ J. L. Smith and Q. Si, cond-mat/9705140; Europhys. Lett. **45**, 228 (1999).
- ⁴ A. M. Sengupta, Phys. Rev. B **61**, 4041 (2000).
- ⁵ L. Zhu and Q. Si, Phys. Rev. B **66**, 024426 (2002); G. Zarand and E. Demler, Phys. Rev. B **66**, 024427 (2002).
- ⁶ Q. Si, S. Rabello, K. Ingersent, and J. L. Smith, Nature **413**, 804 (2001) and Phys. Rev. B **68**, 115103 (2003).
- ⁷ A. Schröder, G. Aeppli, R. Coldea, M. Adams, O. Stockert, H. v. Löhneysen, E. Bucher, R. Ramazashvili, and P. Coleman, Nature **407**, 351 (2000).
- ⁸ D. Withoff and E. Fradkin, Phys. Rev. Lett. **64**, 1835 (1990).
- ⁹ C. R. Cassanello and E. Fradkin, Phys. Rev. B **53**, 15079 (1996) and **56**, 11246 (1997).
- ¹⁰ R. Bulla, T. Pruschke, and A. C. Hewson, J. Phys.: Condens. Matter **9**, 10463 (1997), R. Bulla, M. T. Glossop, D. E. Logan, and T. Pruschke, *ibid* **12**, 4899 (2000).
- ¹¹ C. Gonzalez-Buxton and K. Ingersent, Phys. Rev. B **57**, 14254 (1998).
- ¹² K. Ingersent and Q. Si, Phys. Rev. Lett. **89**, 076403 (2002).
- ¹³ M. Vojta and L. Fritz, cond-mat/0309262.
- ¹⁴ J. Bobroff, W. A. MacFarlane, H. Alloul, P. Mendels, N. Blanchard, G. Collin, and J.-F. Marucco, Phys. Rev. Lett. **83**, 4381 (1999).
- ¹⁵ J. Bobroff, H. Alloul, W. A. MacFarlane, P. Mendels, N. Blanchard, G. Collin, and J.-F. Marucco, Phys. Rev. Lett. **86**, 4116 (2001).
- ¹⁶ M.-H. Julien, T. Feher, M. Horvatic, C. Berthier, O. N. Bakharev, P. Segransan, G. Collin, and J.-F. Marucco, Phys. Rev. Lett. **84**, 3422 (2000).
- ¹⁷ E. H. Kim, Y. B. Kim, and C. Kallin, cond-mat/0205054.
- ¹⁸ S. Sachdev, C. Buragohain and M. Vojta, Science **286**, 2479 (1999).
- ¹⁹ M. Vojta, C. Buragohain and S. Sachdev, Phys. Rev. B **61**, 15152 (2000).
- ²⁰ M. Vojta and M. Kirčan, Phys. Rev. Lett. **90**, 157203 (2003).
- ²¹ S. Sachdev, Physica C **357**, 78 (2001).
- ²² S. Sachdev and J. Ye, Phys. Rev. Lett. **70**, 3339 (1993); A. Georges, O. Parcollet, and S. Sachdev, Phys. Rev. Lett. **85**, 840 (2000) and Phys. Rev. B **63**, 134406 (2001).
- ²³ S. Sachdev, Phys. Rev. B **55**, 142 (1997).
- ²⁴ A. Zawadowski and P. Fazekas, Z. Physik **226**, 235 (1969); P. Coleman, Phys. Rev. B **29**, 3035 (1984).
- ²⁵ T. A. Costi, J. Kroha, and P. Wölfle, Phys. Rev. B **53**, 1850 (1996).
- ²⁶ S. Sachdev, M. Troyer, and M. Vojta, Phys. Rev. Lett. **86**, 2617 (2001).
- ²⁷ S. Sachdev, J. Stat. Phys. **115**, 47 (2004).
- ²⁸ S. Sachdev and M. Vojta, Phys. Rev. B **68**, 064419 (2003).
- ²⁹ E. Brezin, J. C. Le Guillou, and J. Zinn-Justin, in *Phase transitions and critical phenomena*, eds. C. Domb and M. S. Green, Page Bros., Norwich (1996), Vol. 6.
- ³⁰ S. Sachdev, *Quantum Phase Transitions*, Cambridge University Press, Cambridge (1999).
- ³¹ V. Barzykin and I. Affleck, Phys. Rev. B **57**, 432 (1998).
- ³² I. Affleck and A. W. W. Ludwig, Nucl. Phys. B **352**, 849 (1991); *ibid.* **360**, 641 (1991).
- ³³ I. Affleck and A. W. W. Ludwig, Phys. Rev. Lett. **67**, 161 (1991), Phys. Rev. B **48**, 7297 (1993).
- ³⁴ M. Troyer, Prog. Theor. Phys. Supp. **145**, 326 (2002).
- ³⁵ O. P. Sushkov, Phys. Rev. B **62**, 12135 (2000).
- ³⁶ The last line in Eq. (43) corrects an error in the entropy expression given in Ref. 18, where a temperature derivative was missed.
- ³⁷ Based on the ϵ expansion we cannot exclude that the impurity entropy at the FB-CR fixed point is zero for $\epsilon = 1$, while being finite for small ϵ . However, this seems unlikely to us because we see no indications for changes in the fixed-point structure²⁸ in the range $0 < \epsilon < 2$, at least for interacting bosons $g \neq 0$; the case $g = 0$ requires further investigation. Furthermore, the large- N calculation in App. D shows that the entropy for the bosonic Kondo problem is finite for all $0 < \epsilon < 2$, while – interestingly – the local susceptibility is only singular for $0 < \epsilon < 1$ due to $\eta_\chi = \epsilon$ (as at the BF-CR fixed point).
- ³⁸ M. Vojta and R. Bulla, Phys. Rev. B **65**, 014511 (2002).
- ³⁹ P. A. Lee, Phys. Rev. Lett. **71**, 1887 (1993).
- ⁴⁰ S. Burdin, D. R. Grempel, and A. Georges, Phys. Rev. B **66**, 045111 (2002).
- ⁴¹ D. R. Grempel and Q. Si, Phys. Rev. Lett. **91**, 026401 (2003).
- ⁴² P. Sun and G. Kotliar, Phys. Rev. Lett. **91**, 037209 (2003).
- ⁴³ K. Haule, A. Rosch, J. Kroha, and P. Wölfle, Phys. Rev. B **68**, 155119 (2003).
- ⁴⁴ A. Polkovnikov, S. Sachdev, and M. Vojta, Phys. Rev. Lett. **86**, 296 (2001).
- ⁴⁵ E. W. Hudson, S. H. Pan, A. K. Gupta, K. W. Ng, and J. C. Davis, Science **285**, 88 (1999); S. H. Pan, E. W. Hudson, K. M. Lang, H. Eisaki, S. Uchida, and J. C. Davis, Nature **403**, 746 (2000).
- ⁴⁶ O. Parcollet, A. Georges, G. Kotliar, and A. Sengupta, Phys. Rev. B **58**, 3794 (1998).